

SCIENTIFIC REPORTS



OPEN

Identification and characterization of genes involving the early step of Juvenile Hormone pathway in *Helicoverpa armigera*

Wanna Zhang^{1,2}, Long Ma³, Haijun Xiao¹, Chen Liu², Lin Chen², Shaolong Wu⁴ & Gemei Liang²

Juvenile hormones (JHs) are crucial regulators for multiple physiological processes in insects. In the current study, 10 genes in mevalonate pathway involved in JH biosynthesis were identified from *Helicoverpa armigera*. Tissue-specific expression analysis showed that six genes were highly expressed in the head which contained the JH biosynthetic gland (corpora allata). Temporal expression pattern showed that 10 of 12 genes were highly transcribed in the late 2nd-instar when the *in vivo* JH titer reached the peak, indicating a tight correlation between JH titer and the transcription of JH synthetic pathway genes. Moreover, ingestion of methoprene, a JH analogue, significantly suppressed the transcription of nine JH biosynthetic genes and caused a feedback upregulation of the JH degradation enzyme. Particularly, the Acetoacetyl CoA thiolase (*HaAce*) and Farnesyl diphosphate synthase gene 4 (*HaFpps4*) showed high transcript abundance, and their temporal expressions keep pace with JH fluctuations. Further study by RNAi showed that knockdown of *HaFpps4* caused the decrease of JH titer, led to a negative effect on the transcript levels of other genes in JH pathway, and resulted in molting disturbance in larvae. Altogether, these results contribute to our understanding of JH biosynthesis in *H. armigera* and provide target genes for pest control based on JH-dependent regulation.

Juvenile hormones (JHs), synthesized and released by corpora allata (CA) which is located in the stomatogastric nervous system of insect brain¹, are critical hormones involved in the regulation of insect molting and metamorphosis². The molt and metamorphosis of insect larvae is preceded by the induction of JH action, in close cooperation with the regulation of ecdysteroid titers³. Normally, ecdysone causes larvae to molt to the next larval stage at the condition of JH being present, and it induces insect metamorphosis in absence of JH⁴. Recent studies revealed that JH is also involved in multiple other physiological processes during insect life cycle, including phase polyphenism, caste differentiation, diapause, reproduction and many other physiological functions⁵⁻⁷. Considering the extensive involvement of JH, a better knowledge of regulatory mechanisms that underlie the fluctuations of JH titers could help provide a potential method for insect control. Actually, JH analogues, such as methoprene, pyriproxyfen and fenoxycarb, have already been used in pest control, and the growth regulation of parasitic wasps^{8,9}.

Change of JH titer in hemolymph is primarily regulated by the modulation in JH synthesis and catabolism through actions of specific enzymes¹⁰. The complete JH biosynthesis is accomplished by 13 separate enzymatic steps, divided into two metabolic sections (Fig. S1). The first section constitutes the mevalonate pathway, which begins from acetyl-CoA to farnesyl pyrophosphate (FPP) formation. In next section, FPP is finally converted to JH through the intermediates of Farnesal and Farnesoic acid¹¹. The first section is conserved among invertebrates, while the next section is specific to insects. Intermediates in the mevalonate pathway are also needed for the biosynthesis of many important metabolites in plants and animals. In animals, the primary end-product of mevalonate pathway is cholesterol, and most research focuses on this pathway due to the underlying cause of

¹Institute of Entomology, Jiangxi Agricultural University, Nanchang, 330045, China. ²State Key Laboratory for Biology of Plant Diseases and Insect Pests, Institute of Plant Protection, Chinese Academy of Agricultural Sciences, Beijing, 100193, China. ³Jiangxi Key Laboratory of Bioprocess Engineering, Jiangxi Science & Technology Normal University, Nanchang, 330013 China. ⁴China Tobacco Midsouth Agricultural Experimental Station, Changsha, 410128, China. Wanna Zhang and Long Ma contributed equally to this work. Correspondence and requests for materials should be addressed to G.L. (email: gmliang@ippcaas.cn)

cardiovascular disease by cholesterol. In insects, the peculiarity of mevalonate pathway is the capacity to synthesize JH due to the lack of relevant cholesterol synthesis enzymes. In insects, the mevalonate pathway involves eight enzymes and is divided into three steps, utilizing acetyl-CoA to form farnesyl diphosphate¹². Firstly, enzymes of acetoacetyl CoA thiolase (*Ace*), HMG-CoA synthase (*Hmgs*), and HMG CoA reductase (*Hmgr*) are involved in catalyzing three units of acetyl-CoA into mevalonate. Then, mevalonate is converted to isopentenyl diphosphate (*Ipp*) through three enzymatic reactions catalyze by mevalonate kinase (*Mk*), phosphomevalonate kinase (*Pk*), and mevalonate diphosphate decarboxylase (*Dpp*)¹³. Finally, FPP synthase (*Fpps*) generates FPP by completing two sequential couplings: first IPP and dimethylallyl pyrophosphate (DMAPP) can condense in a head-to-tail manner to produce geranyl diphosphate (GPP); subsequently, GPP and IPP are condensed to yield FPP¹². However, it has been difficult to identify the genes encoding enzymes from farnesyl diphosphate to JH because of the lack of vertebrate homologs.

Functional characterizations of enzymes in mevalonate pathway have been elucidated in many insects, such as *Bombyx mori*, *Aedes aegypti*, *Apis mellifera*, *Tribolium castaneum* and *Danaus plexippus*. In *B. mori*, it was found that one type of enzyme in each step of the mevalonate pathway was encoded by a single gene, except for *Fpps*¹⁴. Moreover, most mevalonate enzyme-encoding genes were highly enriched in the CA and their expression patterns correlated with the fluctuation of JH titer^{14,15}. Transcription changes in mevalonate enzyme-encoding genes resulted in an increase or decrease in JH content, indicating a relevant role of these genes in JH biosynthesis. Until recently, enzymes involved in the early steps of JH pathway have been identified in vertebrates and limited in model insect species, and the functional studies are confined to *Hmgs*¹⁶, *Hmgr*^{17,18}, *Ippi*^{19,20} and *Fpps*^{21–25}. However, in agricultural pests, the identification and functional characterization of the mevalonate pathway enzyme encoding genes are poorly understood.

Besides of the involvement in JH biosynthesis, the mevalonate pathway also participates in other processes. For example, the pine engraver beetle *de novo* produces the monoterpenoid pheromone component ipsdienol via the mevalonate pathway²⁶, and the mevalonate enzyme-encoding genes are proposed to be involved in the pheromone production in *Lutzomyia longipalpis*²⁷. Additionally, (E)- β -farnesene, the key component of aphid alarm pheromone components²⁸, iridoid, a defensive secretion in leaf-beetle larvae²⁹, and farnesene, the termite defence secretion³⁰, are all *de novo* synthesized through the mevalonate pathway in insects.

The cotton bollworm, *Helicoverpa armigera*, is one serious pest of cotton, corn, vegetables, and many other crops. Recently, transgenic cotton expressing the Cry-1 Ac gene from *Bacillus thuringiensis* (Bt) has suppressed this pest effectively³¹. However, field-evolved resistance to Cry1 Ac showed a significant increase in northern China³², which has resulted in an urgency to develop novel pest management strategies. The molting process of *H. armigera* is regulated by JH and 20-hydroxyecdysone, and studies revealed that silencing the genes involved in JH pathway blocked the normal metamorphosis process^{33,34}. Obviously, deep insight into the enzyme-regulating mechanisms in JH biosynthetic pathway will provide several promising targets for pest management. In the current study, we identified 10 enzyme-encoding genes in the early steps of JH biosynthetic pathway, and quantified the tissue distribution and developmental profiles of these genes during insect life cycle. Finally, we functionally characterized the silencing effect of *HaFpps4* and *HaAce* on the JH biosynthesis and the response of other genes. This study broadens the knowledge about enzyme-encoding genes involved in the JH pathway in *H. armigera* and provides target genes for pest control based on JH-dependent regulation.

Results

Identification of genes encoding mevalonate pathway enzymes. The mevalonate pathway involved in Juvenile hormone biosynthesis is consisted of eight enzyme reactions. In our study, 10 enzyme-encoding genes were identified: *HaAce*, *HaHmgs*, *HaMk*, *HaPk*, *HaDpp*, *HaIppi*, *HaFpps1*, *HaFpps2*, *HaFpps3* and *HaFpps4* (Table S1). And the gene sequences were listed in Data Set S1. The predicted genomic structures of these genes, as well as *Hmgr*³⁵, were presented in Fig. 1. The genomic structures revealed that no introns were contained in *Hmgs*, *Hmgr* and *Dpp*, while introns which interrupt coding sequences occurred in the rest of genes (Fig. 1).

Fpps, a key enzyme in isoprenoid biosynthesis, catalyzes the final reaction of the mevalonate pathway to generate the precursor of JH. In this study, four transcripts encoding *Fpps* gene were identified in *H. armigera*. Sequence analysis revealed that the *Fpps* family contained several critical domains characteristic for isoprenyl diphosphate synthases, including two aspartate rich motifs named FARM (first aspartic rich motif) and SARM (second aspartic rich motif). However, the SARM domain of *HaFpps1* was slightly different from other *Fpps*, containing a QNDXXD instead of QDDXXD motif (Fig. S2). *Fpps* proteins from 15 insects were used to construct rooted, neighbor-joining phylogenetic trees, which showed that *HaFpps1* was distinct from other sequences. Additionally, *HaFpps2* was clustered with *HaFpps3*, but they were in distinct phylogenetic clusters from *HaFpps4* (Fig. S2). The genomic structure of *HaFpps1* gene was different from that of the other three genes, indicating that five exons were present in *HaFpps1*, while six were present in *HaFpps2*, *HaFpps3* and *HaFpps4* (Fig. 1).

Tissue expression of JH biosynthetic pathway genes in *H. armigera*. The expression profiles of ten identified mevalonate enzyme-encoding genes were investigated, in addition to two relevant genes reported by other literature, *JhAmt* (JH acid methyltransferase) and *Hmgr*³⁵. Results showed that the transcription levels of these genes were consistent with their enzymatic activities in JH biosynthesis (Fig. 2). The expressions of seven genes (*HaAce*, *HaHmgs*, *HaHmgr*, *HaPk*, *HaFpps1*, *HaFpps2* and *JhAmt*) were highly enriched in head where the JH synthetic gland is located. Additionally, *HaMk*, *HaIppi*, *HaFpps3* and *HaFpps4* showed wide tissue distribution. Interestingly, *HaDpp* was widely distributed in multiple tissues, but was significantly higher in fat body ($P < 0.05$). In comparison of the transcript abundance of *Fpps* genes in single tissue, *Fpps4* was significantly higher expressed than the other *Fpps* genes (Fig. S3).

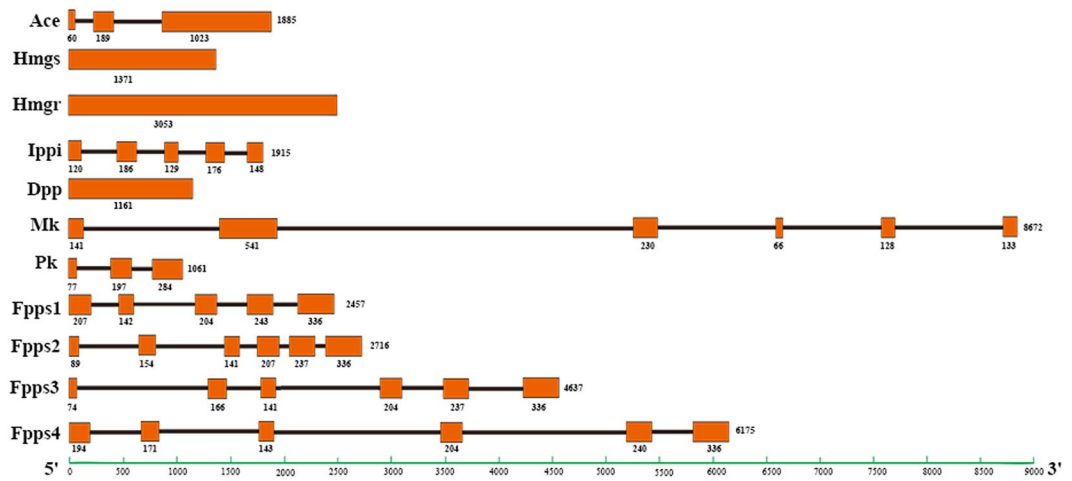


Figure 1. Genomic structure of 11 mevalonate enzymes-encoding genes in *H. armigera*. The saffron rectangles and straight-lines represent the exons and introns, respectively. Nucleotide numbers at the end of the diagram are indicated to provide a general estimation of gene size. The respective length of each exon is labeled under the rectangle.

Expression profiles during developmental stages. The temporal expressions of genes in the mevalonate pathway were shown in Fig. 3. Overall, the transcription levels of mevalonate enzyme-encoding genes were sharply increased in the late 2nd-instar larval (the 3rd day of 2nd-instar, namely 2L-3), showing a transient activation of these enzymes just before the molting of 2nd-instar larvae. And these transcriptions were significantly declined during the 4th- and 5th-instar. Moreover, an increase in transcription was observed in most mevalonate pathway genes at the late pupal stage, except for that of *HaAce*, *HaFpps1* and *HaFpps4*. It was also found that the expression levels of several enzyme-encoding genes in JH biosynthesis, such as *HaHmgs*, *HaMk*, *HaPk*, *HaDpp* and *HaFpps3*, were much higher in pupae and adults, relative to those in 3rd to 5th instar larvae.

Dynamic fluctuations of JH titers during developmental stages. The temporal changes of JH titer during *H. armigera* development was depicted in Fig. 4A. Results showed that the JH biosynthesis remained active in larval stages, but declined at the last larval instar. It was especially interesting that a transient increase of JH titer was observed immediately preceding the molting of each larval instar. The highest JH titer occurred on the 3rd day of 2nd-instar, which correlated well with the high transcriptions of enzymes in mevalonate pathway at the same period (Fig. 3). However, in the prepupal and pupal stages, rare amount of JH was produced. Subsequently, a sharp increase in JH content was observed at late pupal stage. After the emergence of adults, JH synthesis became active again and JH levels peaked at 3rd-day-old adults. Overall, the JH biosynthesis was more active in larval stages compared to that in pupae and adults.

Effects of JHA ingestion on transcript levels of genes in mevalonate pathway. We examined the effect of JHA on expression levels of genes associated with JH biosynthesis (Fig. 4B). After treatment with 2 μg methoprene, the expressions of *HaAce*, *HaHmgs*, *HaMk*, *HaPk*, *HaIppi*, *HaDpp*, *HaFpps3*, *HaFpps4* and *JhAmt* were significantly downregulated, while no significant differences were found in the expression level of *HaHmgr*, *HaFpps1*, *HaFpps2* and Juvenile Hormone Esterase (*HaJhe*). *Jhe* is a crucial carboxylesterase for JH degradation in hemolymph. And the expression of *HaJheh* (Juvenile Hormone Epoxide Hydrolase), playing a pivotal role in JH catabolism in collaboration with *Jhe*, was induced after methoprene treatment (Fig. 4). Results indicated that JHA significantly suppressed the gene expression in JH biosynthesis, while induced the gene expressions in JH catabolic pathway.

Knockdown of *HaFpps4* suppressed the genes expression in mevalonate pathway. As shown in Figs 2, 3 and 4, *HaAce* and *HaFpps4* had high abundance in all tissues, and their peak transcriptions was detected immediately preceding the arrival of the highest JH titer in larval stage, indicating that *HaAce* and *HaFpps4* may play important roles in early step of JH biosynthesis. Therefore, these two genes were selected for in-depth study using RNAi. Results showed that the dsRNA injections significantly decreased the expression levels of target *HaAce* and *HaFpps4* in the tissue of head. Compared to the control group, the expression of *HaAce* was reduced by 78.12%, 77.02% and 81.53% at 48 h, 72 h and 96 h post injection, respectively (Fig. 5A). Similarly, the expression level of *HaFpps4* was reduced by 67.35%, 77.92%, 81.82% and 50.05% at 24 h, 48 h, 72 h and 96 h after dsRNA injection, respectively (Fig. 5B). However, no significant efficacy was detected in the tissue of midgut either in *dsAce* or *dsFpps4* treatment compared to the control group (Fig. 5C,D). In epidermis, the *HaFpps4* expression was significantly reduced at 24 h and 48 h post injection, but the silencing efficacy of *HaAce* lasted only 48 h after dsRNA injection (Fig. 5E,F).

Additionally, knockdown of *HaAce* resulted in the up-regulation of *HaHmgs*, *HaMk*, *HaIppi*, *HaDpp*, *HaFpps4* and *JhAmt*, but no significant change was detected on the JH titer (Fig. 6A,B). When *Fpps4* was silenced, the expressions of *HaAce*, *HaIppi* and *HaJhe* were significantly down-regulated, while *JhAmt* and *HaMk* were

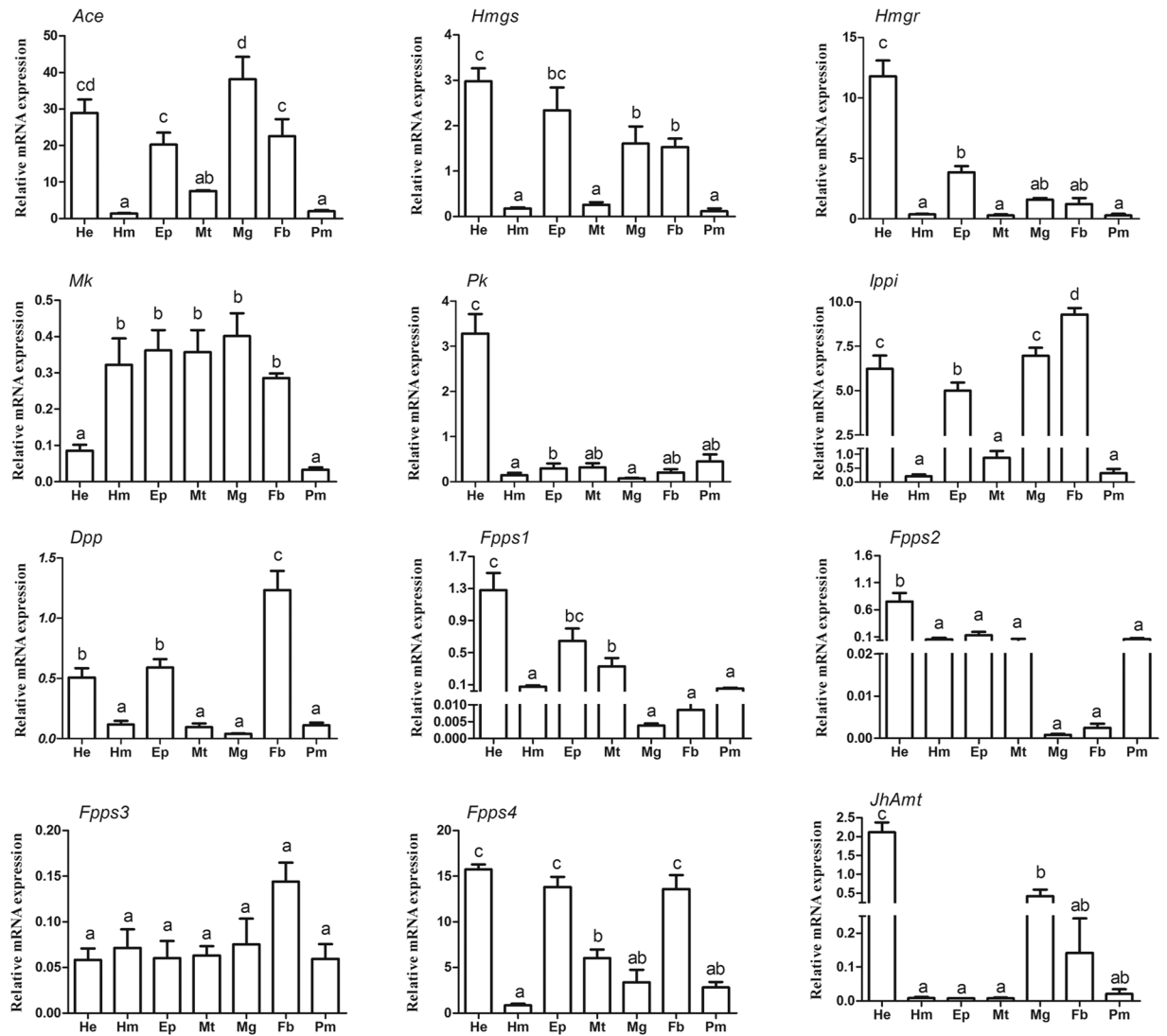


Figure 2. Tissue-specific transcript distribution of 11 mevalonate enzyme-encoding genes and *HaJhAmt* in *H. armigera*, 5th-instar 0 d larvae. He: head; Ep: epidermis; Fb: fat body; Mg: midgut; Mt: malpighian tubules; Hm: hemolymph; Pm: peritrophic matrix. The bars represent the average (\pm SE) of biological repeats. Different letters indicate a significant difference between specimens ($P < 0.05$).

up-regulated, and there was no effect on the expression of *HaHmgs*, *HaDpp* and *HaJheh* (Fig. 6D). In contrast to *HaAce* silencing, the knockdown of *HaFpps4* resulted in a decrease of JH titer *in vivo* relative to the control (Fig. 6E). Moreover, approximately 40% ($n = 72$) of the *HaFpps4* RNAi larvae did not molt normally (Fig. 6F), while no abnormal molting was detected in the ds*HaAce* treatment group. The subcellular localization of *HaFpps4* protein was investigated in Hi5 cell lines. Fluorescence microscopic observations revealed that *HaFpps4* was dispersed in both cytoplasm and cell nucleus (Fig. S4).

Discussion

Juvenile hormones play central roles in regulating many aspects of physiological processes in insects. Changes of JH titers are primarily regulated by modulations in the synthesis of JH, but also by JH catabolism through the action of specific enzymes¹. To understand the regulation mechanisms of JH biosynthesis, it is important to study the enzymes involved in each step of JH biosynthesis, including the enzymes in mevalonate pathway. Multiple JH biosynthetic-related genes have been identified from the genome or transcriptome data in insects, especially in the model insect species³⁶. Whilst the genes encoding JH degrading enzymes and their functions have been fairly well characterized in agricultural pests³⁷, this is not so for the JH biosynthesis steps.

Typically, the mevalonate pathway in most animals would lead to the production of steroids, and the regulatory mechanism of this pathway in vertebrates has been studied exhaustively³⁸. In arthropods, the mevalonate pathway constitutes the initial step of JH biosynthesis, which has lost the ability to synthesize steroids¹¹, and the peculiarities of mevalonate pathway in insects is the capacity to synthesize JH precursor. In this study, we successfully identify 10 mevalonate enzyme-encoding genes from a transcriptome of *H. armigera*. Previously, it

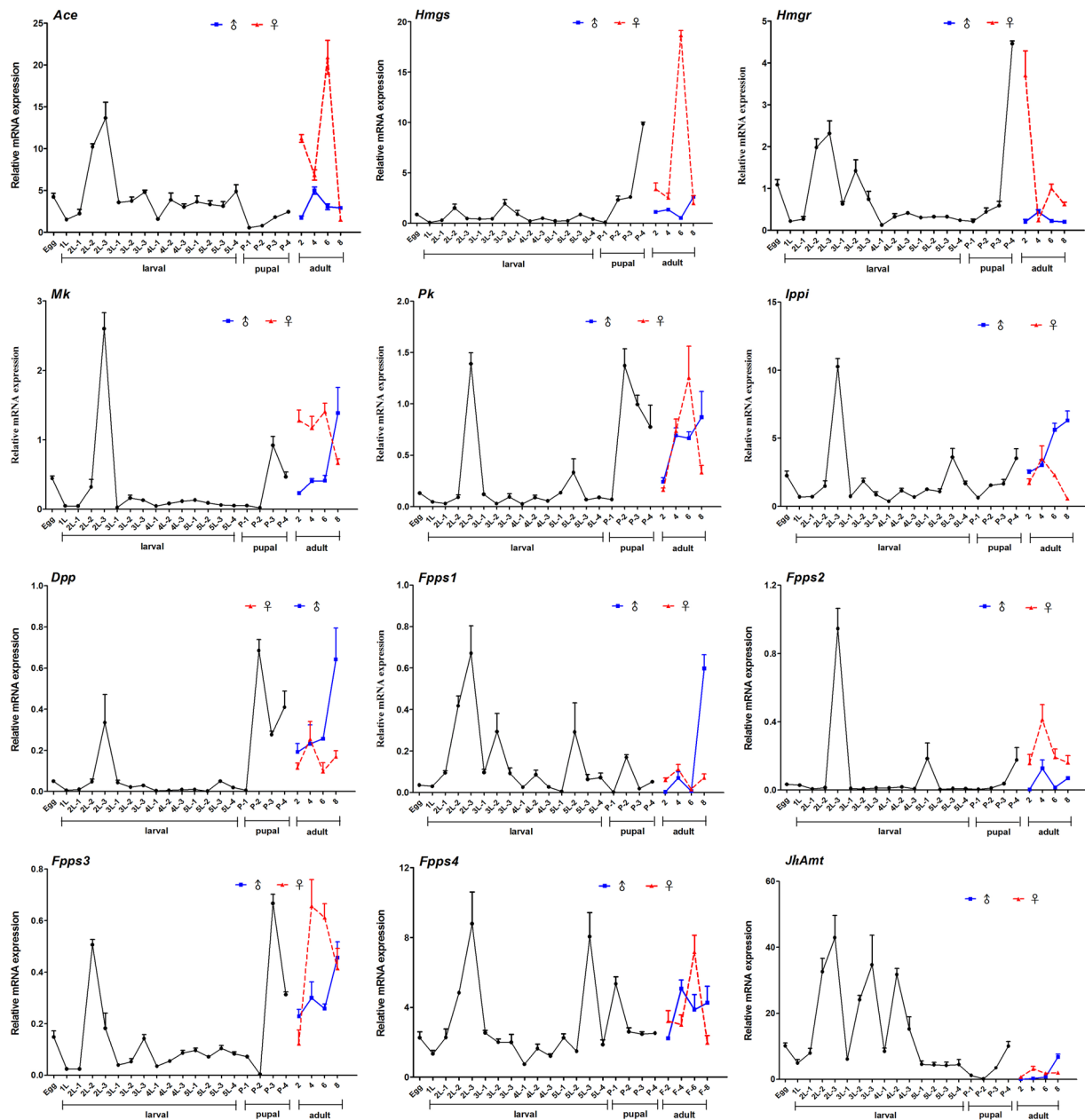


Figure 3. Expression patterns of 11 mevalonate enzyme-encoding genes as well as *JhAmt* in *H. armigera* at different developmental stages. Samples were prepared at an interval of one day during larval stages (1st-, 2nd-, 3rd-, 4th-, and 5th- instar) and two days for adult. Four types of pupae were prepared at the pupal stage (white pupae, green pupae, brown pupae and black pupae). For each sample, three independent pools of 3–50 individuals are measured. The bar represents the average (\pm SE) of the biological repeats.

has been reported that the mevalonate pathway is conserved among invertebrates and consisted of eight typical enzyme-catalyzed steps⁴¹. In our research, it is shown that each enzyme is encoded by a single gene, except for *Fpps*, which is comprised of four homologs. This pattern is similar to the study in *B. mori*¹⁴ and *A. mellifera*³⁹, containing three and six *Fpps* homologs, respectively. However, Li *et al.* found two *Ace* isoforms and two *Hmgr* isoforms in *L. decemlineata*¹⁵. Similarly, two transcripts of *Hmgr* were detected in crustaceans⁴⁰ and two genes encoding *Hmgs* with 78% similarity have been reported in *Blattella germanica*⁴¹.

Since the mevalonate pathway is generally considered as the first step of JH biosynthetic process, it was proposed that some enzymes in this pathway could be rate-limiting enzymes of JH biosynthesis⁴². The tissue expression profiles showed that 6 of the 11 mevalonate pathway genes were highly expressed in the head, similar to that of *JhAmt*. And the high expression of mevalonate enzymes in head can be attributed to the fact that CA is the special gland for the JH synthesis. Meanwhile, genes such as *HaMk*, *HaIppi*, *HaFpps3*, and *HaFpps4* had varied expressions in tissues. And the non-specific tissue distribution of mevalonate enzyme-encoding genes was also found in *A. mellifera*³⁹, *D. punctate*⁴³, *A. aegypti*¹³ and *B. mori*³⁶. This could be due to the fact that some defensive

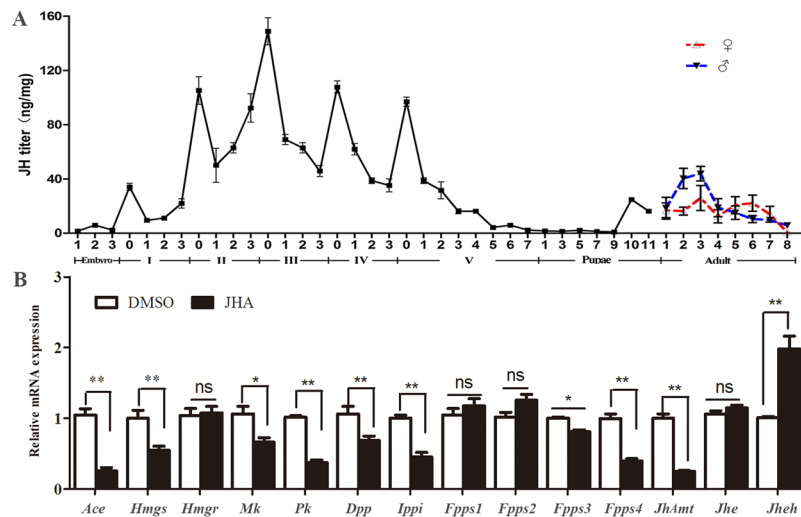


Figure 4. (A) The changes of JH III content *in vivo* of *H. armigera* from embryo to adult stages. Samples were collected daily except for a two-day collection in the pupal stage. (B) Effects of JHA ingestion on transcript levels of genes in mevalonate pathway. The standard error is represented by the error bar. Asterisks indicate statistically significant differences between groups (Student's t-test): * $P < 0.05$, ** $P < 0.01$. ns: no significant difference.

secretions and pheromones in insects are also included in the final products of the mevalonate pathway. In blister beetle *Epicauta chinensis*, the biosynthesis of a defensive toxin, cantharidin, plays a part in chemical defense as well as courtship and mating, is regulated by an enzyme in mevalonate pathway¹⁸. It is not surprising that some mevalonate enzyme-encoding genes have wide tissue expression in *H. armigera* as well as in other insects⁴⁴.

A certain titer of JH is necessary for larvae to maintain the larval state, so in most cases the JH level increases during molting. High titers were found at the beginning of the 3rd, 4th and 5th larval instar in *B. mori*, and in the nymphal stage of *Cryptotermes secundus*, in which the JH titer rose before the next molt and then dropped sharply in both species^{45,46}. In our study, JH levels were fluctuating during the developmental stages, and a transient increase of JH titer was observed right before the molt of each larval instar. The highest JH titer was detected on the 3rd day of the 2nd-instar, while minimal amount of JH was detected in the pupal stage (Fig. 4A). Temporal expression patterns showed that 10 of 12 tested genes were significantly up-regulated in the late 2nd-instar larvae when JH level reached the peak. In the 5th instar, the expression of *JhAmt* and most of the mevalonate enzyme-encoding genes declined to a low level, coupled with the decline in JH biosynthesis. This decline may be due to the shut-down of these genes. In *B. mori*, the levels of *Mk*, *Pk*, *Dpp*, and *Ippi* transcripts were correspondingly low when JH decreased during the pupal stage¹⁴. All these data show a tight correlation between JH titer and transcription regulation of the JH synthetic pathway genes.

Many factors regulate the mevalonate pathway and JH synthesis in insects, and some studies have shown that JH itself is a key regulator of JH pathway. In *L. decemlineata*, the activities of enzymes catalyzing the final step of JH biosynthetic pathway were diminished after JH III treatment⁴⁷. In *Diptera punctata*, the JH synthesis activity of the original CA was reduced when implanted with additional CA or ingested with exogenous JH *in vivo*⁴⁸. Methoprene, an analogue of JH, has been proved to activate JH pathway to regulate gene expression in *Drosophila melanogaster*⁴⁹ and *Nilaparvata lugens*⁵⁰. In our study, ingestion of methoprene significantly suppressed the expression of eight mevalonate enzyme-encoding genes as well as *JhAmt*. Similarly, the expression of *Fpps* was restrained by exogenous JH treatment in *Ips pini*⁴⁴, and *JhAmt* transcription was also repressed in *L. decemlineata*⁵¹. However, in the last-instar larvae of female *B. germanica*, exogenous JH had no effect on *Hmgr* mRNA levels. In our results, no significant change in *Hmgr* levels was detected after JHA application, whereas JH increased the mRNA levels of *Hmgr* and *Hmgs* in *Ips paraconfusus* and *Dendroctonus jeffreyi*^{52,53}. Moreover, we found that ingestion of JHA significantly upregulated the transcription of *Jheh*, and the action of *Jheh* in JH degradation has been explored in certain insects^{54–56}. Actually, the JH titer in insects is controlled by a balance of various processes including synthesis, degradation, sequestration and excretion. Transcription and activities of the biosynthetic and catabolic enzymes in JH pathway are affected when out of balance.

Four different isoforms of *Fpps* were identified in *H. armigera*, which was similar to that in Lepidoptera³⁶ and Hymenoptera³⁹, however, only a single-copy gene was identified in other insect orders^{15,22}. Most insects produce only one chemical form of JH, but the Lepidoptera produce four derivatives that feature ethyl branches. In Lepidoptera, *FPPS*s have long been suspected of exhibiting structural features allowing them to accommodate the bulkier homologous substrates and products used as precursors of ethyl-branched JHs, therefore, it was speculated that the diversity of JH types is linked to the duplication of *Fpps* genes in Lepidoptera insects⁵⁷. Phylogenetic analysis revealed that the *Fpps* family was conserved in insects (Fig. S2) with two aspartate-rich motifs: FARM and SARM. Interestingly, the FARM in most known eukaryotic *Fpps* had two aromatic residues which were not found in FARM of *Fpps* in many insects. A multispecies comparison of *Fpps* genes revealed that only several

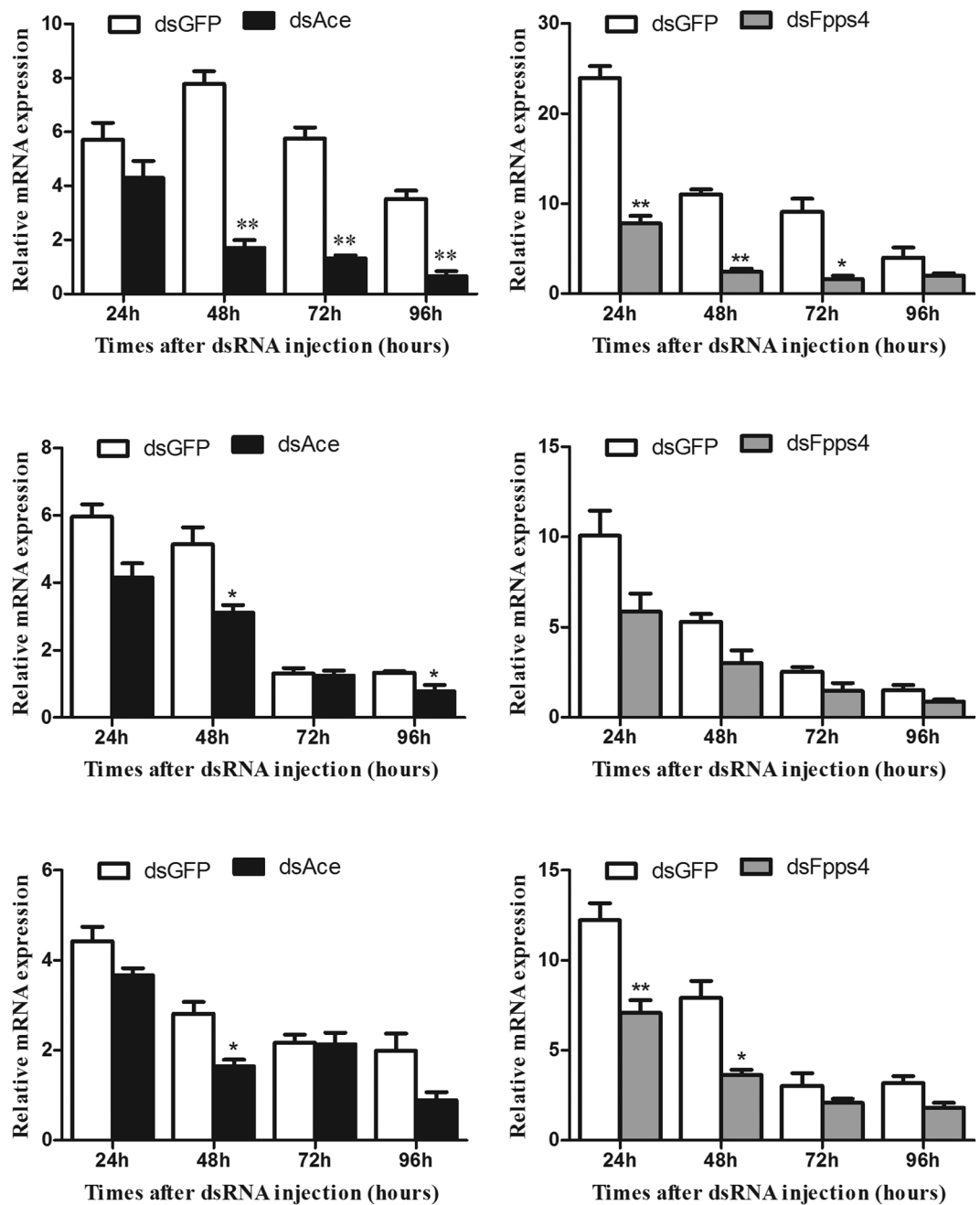


Figure 5. Detection of mRNA levels after dsRNA treatment in the newly molted fourth-instar larvae. *Ace* RNAi efficiency in the head (A), midgut (C) and epidermis (E) from 24 to 96 hours after dsRNA injection. *Fpps4* RNAi efficiency in the head (B), midgut (D) and epidermis (F) from 24 to 96 hours after dsRNA injection. Asterisks indicate statistically significant differences between groups (t-test): *P < 0.05, **P < 0.01.

lepidopteran species contained the NDXXE signature motif⁵⁴, which may have evolved a specialized function in the biosynthesis of JH.

Previously, functional analysis of JH biosynthetic genes was mainly focused on *JhAmt* and *Hmgr*, which have been shown to be essential in insect development and reproduction^{15,16,35,43,58–60}, while few studies were about *Fpps*. In our study, the temporal expression of *HaFpps* was correlated with the changes of JH titer in larval stage due to the fact that their peak transcriptions were right before the arrival of the highest JH titer (Figs 3 and 4). Additionally, we found that knockdown of *HaFpps4* significantly downregulated the transcription of *HaAce*, *HaHmgs*, *HaMk*, *Halppi* and *JhAmt* in *H. armigera*. One possible explanation was that RNAi treatment in *H. armigera* inhibited the production of isoprenoid, an essential JH precursor, resulting in a negative feedback and downregulating the expression of other genes to balance the quantities of intermediates and enzymes. In *A. aegypti*, FPPase efficiently hydrolyzed FPP into farnesol, and silencing of *AaFPPase-1* caused a significant decrease in JH biosynthesis, which strengthened the possibility that FPP acted as the crucial enzyme in regulating

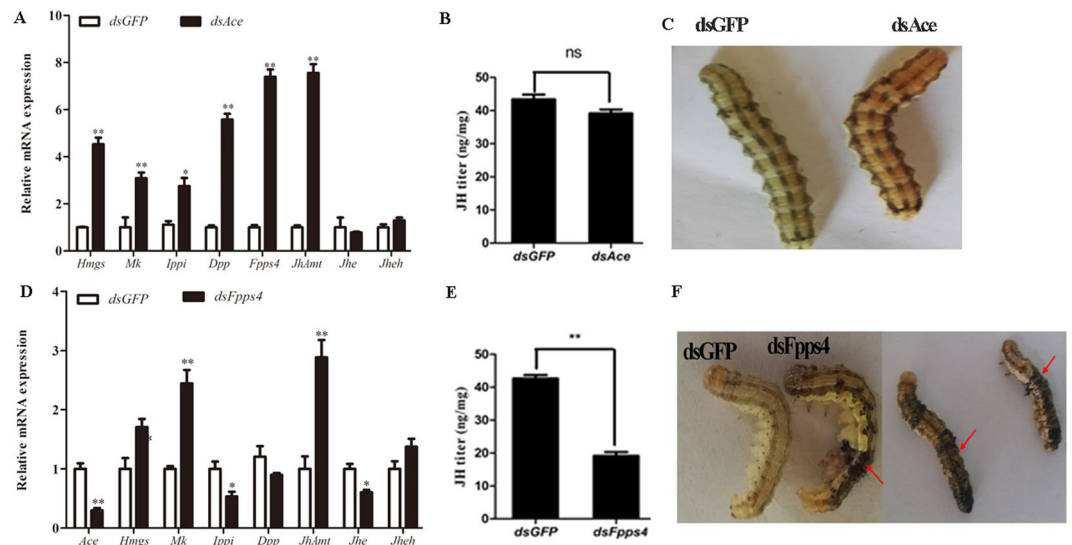


Figure 6. The effects of HaAce RNAi and HaFpps4 RNAi on the larvae. At 1d fourth-instar, larvae were microinjected with dsRNA of HaFpps4 (dsFpps4), dsRNA of HaAce (dsAce) or dsRNA of Green fluorescent protein (dsGFP) (control). The expression levels of the mevalonate pathway genes (A,D), the changes of JH titer (B,E) and the larvae development (C,F) were analyzed. The abnormal molting observed in dsFpps4 injection was labeled with red arrow. The standard error is represented by the error bar. Asterisks indicate statistically significant differences between groups (t-test): * $P < 0.05$, ** $P < 0.01$, ns: no significant difference.

JH synthesis²². Similarly, the activity of *A. aegypti* Mk exhibited efficient feedback inhibition from long-chain isoprenoids, such as geranyl diphosphate and farnesyl diphosphate⁶¹. This study also showed that knockdown of *Fpps4* caused a significant decline in JH titer, leading to the darkening of cuticle and the molting disturbance in larvae (Fig. 6). These data suggest FPP might play a critical role in the synthesis of isoprenoids in insects, and the change of *Fpps* transcription can influence JH biosynthesis.

In conclusion, the mevalonate pathway is essential for the precursor synthesis of JH. Even though data on mevalonate pathway has been characterized in several insect species, there remained many unanswered questions in *H. armigera*. Here, our study annotated 10 genes in mevalonate pathway and investigated the function of particular genes in JH biosynthesis. This paper enriches the knowledge of regulatory mechanisms of JH biosynthesis in *H. armigera*. In addition, the functional analysis of HaFpps4 demonstrated that HaFpps4 played an indispensable role in JH biosynthesis, and was critical for regulating the transcription of JH pathway genes. Given the important role of JH in insect, genes involved in JH biosynthesis could provide potential targets for developing novel insecticide with high selectivity. And our results highlight the potential application of these genes for controlling this pest.

Materials and Methods

Insects. *H. armigera* used in this study were reared in the laboratory at $27 \pm 2^\circ\text{C}$, $75 \pm 10\%$ relative humidity with a photoperiod of 14: 10 (L: D). The larvae were reared on an artificial diet in the 24-well plate, and transferred into 25-ml glass tubes containing an artificial diet at the fifth instar for pupation (one larvae per tube). Adults were fed with 10% sugar solution.

Tissue collection, total RNA isolation, and cDNA synthesis. For developmental expression analysis, individuals at the stages of egg, larvae (first, second, third, fourth and fifth instar), white pupae, green pupae and black pupae were collected, and samples from female and male after emergence were also collected. For tissue-specific expression analysis, tissues (including head, epidermis, fat body, midgut, malpighian tubules, hemolymph, and peritrophic matrix) were dissected from the 5th-instar 0 d larvae in phosphate-buffered saline (PBS). All samples were frozen immediately in liquid nitrogen and stored at -80°C until RNA isolation. Each group contained 3 to 50 individuals and three biological replicates were performed.

Total RNA was extracted using Trizol reagent (Invitrogen, Carlsbad, CA). The quality of each RNA sample was measured by a NanoVue spectrophotometer (GE-Healthcare, Germany) and 1% agarose gel electrophoresis. After the digestion of residual genomic DNA with DNase I (Promega), 2 μg total RNA was reverse transcribed to cDNA with the Fast Quant RT kit (TIANGEN, Beijing, China) according to the instructions.

Confirmation of genes involved in the JH biosynthetic pathway. Specific primers for gene cloning (Table 1) were designed based on homologous sequences identified in our transcriptome database. The sequence information was validated using cDNA of the whole body as templates for PCR. All PCR products were analyzed by 1% agarose gel electrophoresis, ligated with the pMD18-T vector (Takara, Dalian, China), and then transformed into competent *Escherichia coli* cells. After transformation, positive clones were picked for sequencing (BGI Tech).

Primer	Forward primer (5'-3')	Reverse primer (5'-3')	Size
RT-PCR analysis			
Actin	CCGTCCACAATGAAGATCAA	ATCGACAATGTTCCGCATTC	330
Ace	TGGCAACTGTGTTCCAAAAG	GAGAGCATGGCACAAGTGAA	407
Hmgr	GAGCACCGGTATTAAGCTG	CAGAGTTTTGGCATCGGTTT	416
Hmgs	ATGGCAGAAAGGCGATAGTG	TCTGGTGATGCATTGAGGAA	406
Mk	TTACGGGCAAATTCCTTGG	TGATGGAGATCCGTGCATTA	419
Pk	GTTGGGTGACGGAGAGTACA	TCCACCTCCTGTTTCCTTCA	351
Ippi	CGGTGAGAGTGGAAAAGAGG	CAACTCTGGGTCCATCTGGT	413
Dpp	TGACTCTACACACTGGCCTG	TTGGTCCGGCATCAAATGTG	365
Fpps1	GTCTGATGGAAGTCTGCAAAT	GGTCTCTGCTGCCGTAGTATTC	474
Fpps2	CCAGAGAACATAACGGAGGAGA	AGAGATATGGGCAGCTTGTACG	416
Fpps3	AATGGGACAACACTTGGACTTC	GGTAGCCTCAAATCACCGTAA	426
Fpps4	CGAAGCCATCACGAAGTACA	CCTCTGTGACTTGCTGGAT	426
qRT-PCR analysis			
Actin	TGGTATTGCTGACCGTATGC	CTGTTGGAAGGTGGAGAGG	142
Ace	TCCAAAAGGAGAATGGAACG	TCCCCATCAGCATATCCAAT	145
Hmgr	ATCGTGGCCACATTAGCTCT	CATCAGCGGCTTGGTACTCT	133
Hmgs	AAGGCAGAGTGTGGAGCCTA	GCCGGGGAACAGTATGTCTA	112
Mk	ATGCCCTGCAGAATAACCAG	CAGTCCAATAGTTAACTCA	132
Pk	TCTGGAGTTGACGATGTTGC	AACCAGACAGCAATCCCAAT	133
Ippi	CGCTGAAACCACAGACTGAA	TTCCCACGAAGTTGTCCTTC	108
Dpp	TGTATACGGTGGCTTCGTCA	GCATTTACAGCCAGTGTGTA	101
Fpps1	CTGCACACAGCACGATTTCT	TAGTCGCCGAAGTACCGACT	145
Fpps2	AAGGATTGCCAATGTTACGG	ATGGAACCTCCACCTTTCTC	109
Fpps3	CAGGAAGGTGCTTGAACACA	CTGGCCAGCTTGTAGTTTCTC	123
Fpps4	GAGACTGGCAAGCACATTGA	CAGCATTTGTGAAGCCAGCA	123
RNAi analysis			
Ace	TAATACGACTCACTATAGGGTGGCAACTGTGTTCCAAAAG	TAATACGACTCACTATAGGGAGAGCATGGCACAAGTGAA	406
Fpps4	TAATACGACTCACTATAGGGACATCGTAGAAGGCACAGAGA	TAATACGACTCACTATAGGGTCTGTAAAGGCGACAACCTG	519
GFP	TAATACGACTCACTATAGGGGCAACATACGGAAAACCTTACC	TAATACGACTCACTATAGGGTGTGTGGACAGGTAATGGTTG	

Table 1. Primers used in this experiment.

To analyze the genomic structure of identified genes, primer pairs were used to amplify the genome DNA of *H. armigera* (Table S2). Genomic DNA was extracted using TIANamp Genomic DNA kit (TianGen, Beijing, China) following the manufacturer's instructions. PCRs were conducted using the LA Taq polymerase (TaKaRa, Dalian, China). The PCR products were subcloned into the pEasy-T3 vector (TransGen, Beijing, China) and sequenced.

Quantitative real-time PCR. The expression profiles characterizing different developmental stages and tissues were analyzed by quantitative real time PCR (qPCR). The cDNA templates were prepared as described, and primers for qPCR were designed by Beacon Designer 7.9 (Table 1). The reference gene β -actin was employed to calibrate the sample-to-sample variation and normalize the target gene expression. The amplification efficiencies of the tested genes and reference gene (β -actin) were calculated using a gradient dilution of templates. Results showed that the amplification efficiencies for tested genes and reference gene were similar and close to 100%. The qPCR reaction was performed using the SYBR[®] Premix Ex Taq[™] II kit (Takara, Dalian, China) and PCR procedure was as follows: 95 °C for 30 s, followed by 40 cycles of 95 °C for 5 s, and 60 °C for 20 s, and melting curve stage. Negative controls without template were included in each experiment. To check the reproducibility, a total of three biological replicates were analyzed and each biological replicate was assessed three times. Relative expression levels were calculated by the following formula: $R = 2^{-(\Delta Ct_{\text{sample}} - \Delta Ct_{\text{calibrator}})}$, where R is the relative expression level, ΔCt sample is the average difference between the Ct of the gene and the β -actin in the experimental sample, and ΔCt calibrator is the average difference between the Ct of the gene and the β -actin in the calibrator. A representative sample was set as the calibrator. All methods and data followed guideline of the MIQE (Minimum Information for publication of Quantitative real time PCR Experiments)⁶².

Quantitative determination of JH. To determine the JH levels, individuals at the different stages were sampled just as that for qPCR analysis. For JH extraction and JH determination, the methods were operated as described in previous paper⁶³. Briefly, the samples were weighed and frozen immediately in liquid nitrogen. Then the samples were homogenized by grinding in 0.9 ml of methanol/isooctane (1:1, v/v), and subsequently adding 1 ml of n-hexane. The resulting suspension was treated with ultrasound (100KHZ) for 5 min and further centrifuged (10 min, 12,000 × g at 4 °C). Next, the hexane (upper) phase was removed by pipette. Another 1 ml of n-hexane was added to the tube and treated ultrasonically before centrifugation and the removal of the hexane (upper) phase. This process was repeated three times. The hexane phase was then ready to dry completely under

Termovap Nitrogen Sample Concentrator (HP-5016SY). Finally, 500 μ l of MeOH was added as a solvent, and the samples were stored at -80°C . Six parallel samples were prepared as the biological replicates.

At first, a five-point calibration curve of JH III (Sigma, USA) was used as the standard (Figs S6–S7). Level of JH III was measured using high performance liquid chromatography (HPLC) (1200 series, Agilent Technologies, San Jose, CA) and the system was operated using LC 3D B.04 software. Chromatographic separation was carried out at 30°C in the isocratic mode using methanol (waters) (80:20, v/v) as the mobile phase. The injection volume was 20 μ l in partial loop with needle overflow. The column used was a reverse phase C18 chromatographic column (ZORBAX SB-C18, 250 nm \times 4.6 nm, Agilent Technologies) at a flow rate of 800 μ l/min. A total separation of 30 min was needed. Each measurement is performed three times.

Effects of methoprene application on genes transcription. The JH analogue methoprene was used to analyze whether JH could affect the transcription of genes in JH synthetic pathway. Methoprene was selected because of its ability to trigger many of the same responses as JH, and it was more stable in hemolymph therefore prolonging the physiological effects. Methoprene stock was diluted to 5 mg/ml with DMSO, and 1 μ l methoprene solution (2 mg/ml) was injected into the newly molted 4th instar larvae (2 μ g/larva). In the same way, an equivalent volume of DMSO was injected into the control group larvae. Each group contained at least 30 individuals with three biological replicates. To determine the effect of methoprene on transcription response in the JH biosynthesis pathway, total RNA from the head tissues in both the hormone treatment and control group was extracted at 24 h after injection, and qPCR assay was performed as before.

Synthesis of dsRNA and RNA interference. Synthesis and microinjections of dsRNA were performed as previously described⁶⁴. In short, target fragments of HaFpps4, HaAce and GFP (green fluorescent protein) for dsRNA synthesis were amplified using specific primers. The PCR products were sub-cloned into the pGEM-T vector and used as templates for target sequence amplification. The dsRNAs were synthesized *in vitro* using a HiScribe™ T7 Transcription Kit system (New England BioLabs, Ipswich, MA) with specific primers fusing the T7 promoter at the 5' end and dissolved in DEPC water. The purity and yield of the dsRNA was checked on a 1.0% agarose gel and a spectrophotometer, respectively. The primers used for dsRNA synthesis are presented in Table 1.

In each knockdown experiment, 60 individuals of newly molted 4th-instar larvae were cold-anesthetized, and 5 μ g single dsRNA solution (dsHaFpps4, dsHaAce or dsGFP) was injected into the abdomen of each larva using a microsyringe (Hamilton, Bonaduz, Switzerland). Each treatment was performed with three biological replicates. Subsequently, ten individuals were randomly selected at 24 h, 48 h, 72 h and 96 h after injection, then the tissues of head, epidermis and midgut were dissected. To investigate the RNAi efficiency, qPCR analysis was performed as mentioned, and the levels of JH were measured to assess the effect of RNAi on JH biosynthesis.

Expression of HaFpps4 genes in insect cells. The *Trichoplusia ni* BTI-Tn-5B1-4 (Hi5) cell line was employed to investigate the subcellular localization of HaFpps4. Cells were incubated in Grace's insect cell culture medium (Life Technologies Co., Grand Island, NY) supplemented with 10% fetal bovine serum (Life Technologies Co., Australia), 100 unit/ml penicillin, and 100 mg/ml streptomycin (Life Technologies Co., Grand Island, NY) at 28°C ⁶⁵.

The whole open reading frame of *HaFpps4* gene was amplified and ligated with the pGEM-T vectors. The target fragment was excised with restriction enzymes (Table 1) from the recombinant plasmid, and then sub-cloned into the plasmid p-EGFP-N1 at the corresponding sites to generate plasmids pHaFpps4-GFP. The Hi5 cells were dispensed into 6-well plates (Corning, USA) at the density of 1×10^6 cells/well and grown overnight. The recombinant plasmid of pHaFpps4-GFP was transfected into Hi5 cells at 2 mg/well using cell-fectin reagent (Life Technologies), as previously reported. At 24 h after transfection, cells expressing recombinant proteins were washed with phosphate-buffered saline, fixed in 4% paraformaldehyde for 20 min, and stained with Hoechst 33342 (1 μ g/ml) for 20 min at room temperature. Then, cells were photographed using an inverted fluorescence Nikon microscope (TE2000-S, Japan).

Data analysis. All the data in this study are presented as means \pm SE. Significant differences were determined by one tailed student t-test or one-way analysis of variance (ANOVA) followed by a least significant difference test (LSD) for mean comparison. All statistical analysis was performed with SAS 9.20 software (SAS Institute, Cary, NC).

References

1. Goodman, W. G. & Cusson, M. In *Insect Endocrinology* (ed. Lawrence, I Gilbert) 310–365 (2012).
2. Riddiford, L. M. In *Metamorphosis* (eds Lawrence, I., Gilbert, Jamshed, R. Tata & Burr, G. Atkinson) 223–251 (1996).
3. Mizoguchi, A. Effects of juvenile hormone on the secretion of prothoracicotropic hormone in the last- and penultimate-instar larvae of the silkworm *Bombyx mori*. *J Insect Physiol.* **47**, 767–775 (2001).
4. Riddiford, L. M., Truman, J. W., Mirth, C. K. & Shen, Y. C. A role for juvenile hormone in the prepupal development of *Drosophila melanogaster*. *Development* **137**, 1117–1126 (2010).
5. Denlinger, D. L. In *Endocrinology II* (ed. L. I. Gilbert) 353–412 (Pergamon, 1985).
6. Riddiford, L. M., Hiruma, K., Zhou, X. & Nelson, C. A. Insights into the molecular basis of the hormonal control of molting and metamorphosis from *Manduca sexta* and *Drosophila melanogaster*. *Insect Biochem Mol Biol.* **33**, 1327–1338 (2003).
7. Jindra, M., Palli, S. R. & Riddiford, L. M. The juvenile hormone signaling pathway in insect development. *Annu Rev Entomol* **58**, 181–204 (2013).
8. Moshitzky, P. & Morin, S. Bemisia tabaci females from the Mediterranean (Q) species detect and avoid laying eggs in the presence of pyriproxyfen, a juvenile hormone analogue. *Pest Manag Sci* **70**, 1468–1476 (2014).
9. Wang, Q. L. & Liu, T. X. Effects of Three Insect Growth Regulators on *Encarsia formosa* (Hymenoptera: Aphelinidae), an Endoparasitoid of *Bemisia tabaci* (Hemiptera: Aleyrodidae). *J Econ Entomol* **109**, 2290–2297 (2016).
10. Noriega, F. G. *et al.* Comparative genomics of insect juvenile hormone biosynthesis. *Insect Biochem Mol Biol* **36**, 366–374 (2006).

11. Belles, X., Martin, D. & Piulachs, M. D. The mevalonate pathway and the synthesis of juvenile hormone in insects. *Annu Rev Entomol* **50**, 181–199 (2005).
12. Noriega, F. G. Juvenile Hormone Biosynthesis in Insects: What Is New, What Do We Know, and What Questions Remain? *International Scholarly Research Notices* **2014**, 1–16 (2014).
13. Nouzova, M., Edwards, M. J., Mayoral, J. G. & Noriega, F. G. A coordinated expression of biosynthetic enzymes controls the flux of juvenile hormone precursors in the corpora allata of mosquitoes. *Insect Biochem Mol Biol.* **41**, 660–669 (2011).
14. Kinjoh, T. *et al.* Control of juvenile hormone biosynthesis in *Bombyx mori*: cloning of the enzymes in the mevalonate pathway and assessment of their developmental expression in the corpora allata. *Insect Biochem Mol Biol.* **37**, 808–818 (2007).
15. Li, Q., Meng, Q. W., Lu, F. G., Guo, W. C. & Li, G. Q. Identification of ten mevalonate enzyme-encoding genes and their expression in response to juvenile hormone levels in *Leptinotarsa decemlineata* (Say). *Gene* **584**, 136–147 (2016).
16. Martínez-González, J., Buesa, C., Piulachs, M.-D., Belles, X. & Hegardt, F. G. Molecular cloning, developmental pattern and tissue expression of 3-hydroxy-3-methylglutaryl coenzyme A reductase of the cockroach *Blattella germanica*. *Eur J Biochem* **213**, 233–241 (1993).
17. Duportets, L., Belles, X., Rossignol, F. & Couillaud, F. Molecular cloning and structural analysis of 3-hydroxy-3-methylglutaryl coenzyme A reductase of the moth *Agrotis ipsilon*. *Insect Mol Biol* **9**, 385–392 (2000).
18. Lü, S., Jiang, M., Huo, T., Li, X. & Zhang, Y. 3-hydroxy-3-methyl glutaryl coenzyme A reductase: an essential actor in the biosynthesis of cantharidin in the blister beetle *Epicauta chinensis* Laporte. *Insect Mol Biol* **25**, 58–71 (2016).
19. Diaz, M. E. *et al.* Characterization of an isopentenyl diphosphate isomerase involved in the juvenile hormone pathway in *Aedes aegypti*. *Insect Biochem Mol Biol.* **42**, 751–757 (2012).
20. Sen, S. E. *et al.* Cloning, expression and characterization of lepidopteran isopentenyl diphosphate isomerase. *Insect Biochem Mol Biol.* **42**, 739–750 (2012).
21. Sen, S. E. *et al.* Purification, properties and heteromeric association of type-1 and type-2 lepidopteran farnesyl diphosphate synthases. *Insect Biochem Mol Biol.* **37**, 819–828 (2007).
22. Nyati, P. *et al.* Farnesyl phosphatase, a corpora allata enzyme involved in juvenile hormone biosynthesis in *Aedes aegypti*. *PLoS one* **8**, e71967 (2013).
23. Zha, S. *et al.* Cloning and functional analysis of farnesyl diphosphate synthase (FPPS) gene from *Mylabris cichorii*. *Biotechnology and Applied Biochemistry*, <https://doi.org/10.1002/bab.1494> (2016).
24. Xu, B. *et al.* Sublethal effects of chlorantraniliprole on juvenile hormone levels and mRNA expression of JHAMT and FPPS genes in the rice stem borer, *Chilo suppressalis*. *Pest Manag Sci*, <https://doi.org/10.1002/ps.4586> (2017).
25. Rivera-Perez, C., Nyati, P. & Noriega, F. G. A corpora allata farnesyl diphosphate synthase in mosquitoes displaying a metal ion dependent substrate specificity. *Insect Biochem Mol Biol.* **64**, 44–50 (2015).
26. Keeling, C. I., Blomquist, G. J. & Tittiger, C. Coordinated gene expression for pheromone biosynthesis in the pine engraver beetle, *Ips pini* (Coleoptera: Scolytidae). *The Science of Nature* **91**, 324–328 (2004).
27. González-Caballero, N. *et al.* Expression of the mevalonate pathway enzymes in the *Lutzomyia longipalpis* (Diptera: Psychodidae) sex pheromone gland demonstrated by an integrated proteomic approach. *Journal of Proteomics* **96**, 117–132 (2014).
28. Vandermoten, S., Mescher, M. C., Francis, F., Haubruge, E. & Verheggen, F. J. Aphid alarm pheromone: An overview of current knowledge on biosynthesis and functions. *Insect Biochem Mol Biol.* **42**, 155–163 (2012).
29. Burse, A. *et al.* Implication of HMGR in homeostasis of sequestered and de novo produced precursors of the iridoid biosynthesis in leaf beetle larvae. *Insect Biochem Mol Biol.* **38**, 76–88 (2008).
30. Hojo, M., Matsumoto, T. & Miura, T. Cloning and expression of a geranylgeranyl diphosphate synthase gene: insights into the synthesis of termite defence secretion. *Insect Mol Biol* **16**, 121–131 (2007).
31. Lu, Y., Wu, K., Jiang, Y., Guo, Y. & Desneux, N. Widespread adoption of Bt cotton and insecticide decrease promotes biocontrol services. *Nature* **487**, 362–365 (2012).
32. Carrière, Y., Fabrick, J. A. & Tabashnik, B. E. Can pyramids and seed mixtures delay resistance to Bt Crops? *Trends in Biotechnology* **34**, 291–302 (2016).
33. Tian, G. *et al.* Transgenic cotton plants expressing double-stranded RNAs target HMG-CoA reductase (HMGR) gene inhibits the growth, development and survival of cotton bollworms. *Int J Biol Sci.* **11**, 1296–1305 (2015).
34. Xiong, Y. H., Zeng, H. M., Zhang, Y. L., Xu, D. W. & Qiu, D. W. Silencing the HaHR3 gene by transgenic plant-mediated RNAi to disrupt *Helicoverpa armigera* development. *Int J Biol Sci.* **9**, 370–381 (2013).
35. Wang, Z. J., Dong, Y., Desneux, N. & Niu, C. RNAi silencing of the HaHMG-CoA reductase gene inhibits oviposition in the *Helicoverpa armigera* cotton bollworm. *PLoS one* **8**, e67732 (2013).
36. Cheng, D. *et al.* Microarray analysis of the juvenile hormone response in larval integument of the silkworm, *Bombyx mori*. *Int J Genomics* **2014**, 426025 (2014).
37. Khalil, S. M. S., Anspaugh, D. D. & Michael Roe, R. Role of juvenile hormone esterase and epoxide hydrolase in reproduction of the cotton bollworm, *Helicoverpa zea*. *J Insect Physiol.* **52**, 669–678 (2006).
38. Mullen, P. J., Yu, R., Longo, J., Archer, M. C. & Penn, L. Z. The interplay between cell signalling and the mevalonate pathway in cancer. *Nat Rev Cancer* **16**, 718–731 (2016).
39. Bomtorin, A. D. *et al.* Juvenile hormone biosynthesis gene expression in the corpora allata of honey bee (*Apis mellifera* L.) female castes. *PLoS one* **9**, e86923 (2014).
40. Li, S. *et al.* David W. The lobster mandibular organ produces soluble and membrane-bound forms of 3-hydroxy-3-methylglutaryl-CoA reductase. *Biochemical Journal* **381**, 831–840 (2004).
41. Buesa, C. *et al.* *Blattella germanica* has two HMG-CoA synthase genes. Both are regulated in the ovary during the gonadotrophic cycle. *J Biologic Chem.* **269**, 11707–11713 (1994).
42. Debernard, S., Rossignol, F. & Couillaud, F. The HMG-CoA reductase inhibitor fluvastatin inhibits insect juvenile hormone biosynthesis. *General and comparative endocrinology* **95**, 92–98 (1994).
43. Huang, J., Marchal, E., Hult, E. F. & Tobe, S. S. Characterization of the juvenile hormone pathway in the viviparous cockroach, *Diploptera punctata*. *PLoS one* **10**, e0117291 (2015).
44. Seybold, S. J. & Tittiger, C. Biochemistry and molecular biology of de novo isoprenoid pheromone production in the scolytidae. *Annu Rev Entomol* **48**, 425–453 (2003).
45. Niimi, S. & Sakurai, S. Development changes in juvenile hormone and juvenile hormone acid titers in the hemolymph and *in-vitro* juvenile hormone synthesis by corpora allata of the silkworm, *Bombyx mori*. *J Insect Physiol.* **43**, 875–884 (1997).
46. Korb, J., Hoffmann, K. & Hartfelder, K. Molting dynamics and juvenile hormone titer profiles in the nymphal stages of a lower termite, *Cryptotermes secundus* (Kalotermitidae)-signatures of developmental plasticity. *J Insect Physiol.* **58**, 376–383 (2012).
47. Khan, M. A., Koopmanschap, A. B. & de Kort, C. A. D. The effects of juvenile hormone, 20-hydroxyecdysone and precocene II on activity of corpora allata and the mode of negative-feedback regulation of these glands in the adult Colorado potato beetle. *J Insect Physiol.* **28**, 995–1001 (1982).
48. Tobe, S. S. & Stay, B. Modulation of juvenile hormone synthesis by an analogue in the cockroach. *Nature* **281**, 481–482 (1979).
49. Restifo, L. L. & Wilson, T. G. A juvenile hormone agonist reveals distinct developmental pathways mediated by Ecdysone-inducible broad complex transcription factors. *Developmental Genetics* **22**, 141–159 (1998).
50. Jin, M. N., Xue, J., Yao, Y. & Lin, X. D. Molecular characterization and functional analysis of Krüppel-homolog 1 (Kr-h1) in the Brown Planthopper, *Nilaparvata lugens* (Stål). *J Integra Agricul.* **13**, 1972–1981 (2014).

51. Fu, K. Y. *et al.* Knockdown of juvenile hormone acid methyl transferase severely affects the performance of *Leptinotarsa decemlineata* (Say) larvae and adults. *Pest Manag Sci* **72**, 1231–1241 (2016).
52. Tittiger, C., Blomquist, G. J., Ivarsson, P., Borgeson, C. E. & Seybold, S. J. Juvenile hormone regulation of HMG-R gene expression in the bark beetle *Ips paraconfusus* (Coleoptera: Scolytidae): implications for male aggregation pheromone biosynthesis. *Cell Mol Life Sci* **55**, 121–127 (1999).
53. Tittiger, C. *et al.* Isolation and endocrine regulation of an HMG–CoA synthase cDNA from the male Jeffrey pine beetle, *Dendroctonus jeffreyi* (Coleoptera: Scolytidae). *Insect Biochem Mol Biol.* **30**, 1203–1211 (2000).
54. Lü, F. G., Fu, K. Y., Guo, W. C. & Li, G. Q. Characterization of two juvenile hormone epoxide hydrolases by RNA interference in the Colorado potato beetle. *Gene* **570**, 264–271 (2015).
55. Tusun, A. *et al.* Juvenile hormone epoxide hydrolase: a promising target for hemipteran pest management. *Sci Rep* **7**, 789 (2017).
56. Zhao, J., Zhou, Y., Li, X., Cai, W. & Hua, H. Silencing of juvenile hormone epoxide hydrolase gene (*Nljeh*) enhances short wing formation in a macropterous strain of the brown planthopper, *Nilaparvata lugens*. *J Insect Physiol* **102**, 18–26 (2017).
57. Cusson, M. *et al.* Characterization and tissue-specific expression of two lepidopteran farnesyl diphosphate synthase homologs: Implications for the biosynthesis of ethyl-substituted juvenile hormones. *Proteins: Structure, Function, and Bioinformatics* **65**, 742–758 (2006).
58. Shinoda, T. & Itoyama, K. Juvenile hormone acid methyltransferase: a key regulatory enzyme for insect metamorphosis. *Proc Natl Acad Sci USA* **100**, 11986–11991 (2003).
59. Li, W. *et al.* Molecular cloning and characterization of juvenile hormone acid methyltransferase in the honey bee, *Apis mellifera*, and its differential expression during caste differentiation. *PLoS one* **8**, e68544 (2013).
60. Mayoral, J. G. *et al.* Molecular and functional characterization of a juvenile hormone acid methyltransferase expressed in the corpora allata of mosquitoes. *Insect Biochem Mol Biol.* **39**, 31–37 (2009).
61. Nyati, P., Rivera-Perez, C. & Noriega, F. G. Negative feedbacks by isoprenoids on a mevalonate kinase expressed in the corpora allata of mosquitoes. *PLoS one* **10**, e0143107 (2015).
62. Bustin, S. A. *et al.* The MIQE Guidelines: Minimum Information for publication of quantitative Real-Time PCR experiments. *Clinical Chemistry* **55**, 611 (2009).
63. Zhang, W. N. *et al.* Reproductive cost associated with juvenile hormone in Bt-resistant strains of *Helicoverpa armigera* (Lepidoptera: Noctuidae). *J Econ Entomol* **109**, 2534–2542 (2016).
64. Zhang, W. N. *et al.* Molecular characterization and function analysis of the vitellogenin receptor from the cotton bollworm, *Helicoverpa armigera* (Hubner) (Lepidoptera, Noctuidae). *PLoS one* **11**, e0155785 (2016).
65. Chen, Z. *et al.* Endogenous expression of a Bt toxin receptor in the Cry1 Ac-susceptible insect cell line and its synergistic effect with cadherin on cytotoxicity of activated Cry1 Ac. *Insect Biochem Mol Biol.* **59**, 1–17 (2015).

Acknowledgements

This research was supported by the Key Project for Breeding Genetically Modified Organisms (grant number 2016ZX08011–002), the National Natural Science Foundation of China (grant number 31621064), the Science and Technology Program of Department of Education of Jiangxi Province (GJJ160354) and Natural Science Foundation of Jiangxi Province of China (20171BAB214028).

Author Contributions

G.-M.L. and W.-N.Z. designed the study. W.-N.Z. and L.M. performed the experiments. G.-M.L., W.-N.Z. and L.M. analyzed the data and wrote the manuscript. H.-J.X., C.L., L.C. and S.-L.W. provided help for performing the experiments. G.-M.L., W.-N.Z. and L.M. shared in the scoping and writing responsibilities. All authors have read and approved the manuscript for publication.

Additional Information

Supplementary information accompanies this paper at <https://doi.org/10.1038/s41598-017-16319-z>.

Competing Interests: The authors declare that they have no competing interests.

Publisher's note: Springer Nature remains neutral with regard to jurisdictional claims in published maps and institutional affiliations.



Open Access This article is licensed under a Creative Commons Attribution 4.0 International License, which permits use, sharing, adaptation, distribution and reproduction in any medium or format, as long as you give appropriate credit to the original author(s) and the source, provide a link to the Creative Commons license, and indicate if changes were made. The images or other third party material in this article are included in the article's Creative Commons license, unless indicated otherwise in a credit line to the material. If material is not included in the article's Creative Commons license and your intended use is not permitted by statutory regulation or exceeds the permitted use, you will need to obtain permission directly from the copyright holder. To view a copy of this license, visit <http://creativecommons.org/licenses/by/4.0/>.

© The Author(s) 2017